Spatial Distribution of Malate Dehydrogenase in Chitosan Scaffolds

Georgianna L. Martin,[†] Shelley D. Minteer,[‡] and Michael J. Cooney*[,†]

Hawaii Natural Energy Institute, University of Hawaii, Honolulu, Hawaii 96822, and Department of Chemistry, St. Louis University, St. Louis, Missouri 63103

ABSTRACT In this work, confocal laser scanning microscopy was used to study the spatial distribution of malate dehydrogenase immobilized within three-dimensional macroporous chitosan scaffolds. The scaffolds were fabricated from solutions of native and hydrophobically modified chitosan polymer through the process of thermally induced phase separation. The hydrophobically modified chitosan is proposed to possess amphiphilic micelles into which the enzyme can be encapsulated and retained. To test this theory, we applied the immobilization procedure of Klotzbach and co-workers [*J. Membr. Sci.* **2006**, *282* (1−2), 276−283] to solutions of fluorophore-tagged malate dehydrogenase in the presence of native and hydrophobically modified chitosan polymer and then tracked the distribution of enzymes in the resulting scaffolds using fluorescent microscopy. Results suggest that the modified chitosan does encapsulate the enzyme with a significant degree of retention and with altered distribution patterns, suggesting that hydrophobic modification of the chitosan polymer backbone does create amphiphilic regions that are capable of physically encapsulating and retaining enzymes. Commentary is also given on how this information can be correlated to enzyme activity and spatial distribution during immobilization processes.

KEYWORDS: enzyme immobilization and distribution • fluorescence • chitosan polymer • confocal laser scanning microscopy

INTRODUCTION

Within the field of enzyme immobilization, the importance of enzyme distribution throughout an immobilization matrix that provides an appropriate chemical microenvironment is well recognized. Minoofar and co-workers, for example, noted the importance of molecular distribution within separate regions of silica gels when using surfactant-directed self-assembly (2). Bru and co-workers noted the importance of the amphiphilic micellar structure to enzyme stability (3, 4), an observation later reinforced by several publications on the hydrophobic modification of Nafion and chitosan polymers to create amphiphilic micelles that stabilize a range of enzymes (5, 6).

It is not surprising then that the application of enzyme entrapment technologies generally assumes that the enzymes are homogenously distributed throughout the immobilization matrix and within favorable chemical microenvironments. The majority of immobilization procedures using polymers either entraps or encapsulates the enzyme. With entrapment, the enzymes are physically retained on a surface by a polymer coating (7−9). When encapsulated, the enzymes are physically retained within mesopore-scale amphiphilic micelles (1). Typically referred to as micellar regions, these micelles are hypothesized to possess mixed hydrophobic and hydrophilic regions, the composition of which can be manipulated by chemical modification of the polymer. The modified polymer can then be fabricated into various two- (2D) and three-dimensional (3D) structures such as macroporous scaffolds (8, 10, 11). Despite a paucity of supporting literature, the assumption that the enzymes are homogenously distributed and sequestered within unique chemical microenvironments that support optimal activity and lifetime is generally held regardless of the process used to mold the modified polymer into various 2D and 3D structures.

Recent work, however, using fluorescent tags has suggested that these assumptions cannot be assumed and that the final distribution of both the chemical microenvironments and enzymes is dependent upon the polymer, its interaction with the enzyme as a charged species, and the immobilization process. Konash and co-workers, for example, demonstrated that the distribution of fluorophore-tagged enzymes was not homogenously distributed within Eastman AQ55 polymer when the drop-cast technique was used to fabricate films, presumably because in the absence of direct anchoring to the polymer the enzymes followed the movement of the aqueous water phase (12). They also showed that the patterned distribution was altered when Nafion and chitosan polymers were used. Their results cast doubt upon the implicit assumption of a homogeneous distribution of enzymes within immobilization polymers, regardless of the technology used to fabricate the polymer into 2D and 3D structures (e.g., the chemical or electrochemical polymerization of a polymer from solution to a solid matrix or the formation of a hydrogel in which the organic or inorganic species precipitates into a solid phase from the enzyme held in the aqueous phase).

To address these concerns, this work presents the application of fluorescence microscopy to track the distribution of malate dehydrogenase (MDH) immobilized within native

* Corresponding author. E-mail: mcooney@hawaii.edu.
Received for review September 25, 2008 and accepted December 17, 2008
[†] University of Hawaii.
[‡] St. Louis University.
DOI: 10.1021/am800077t

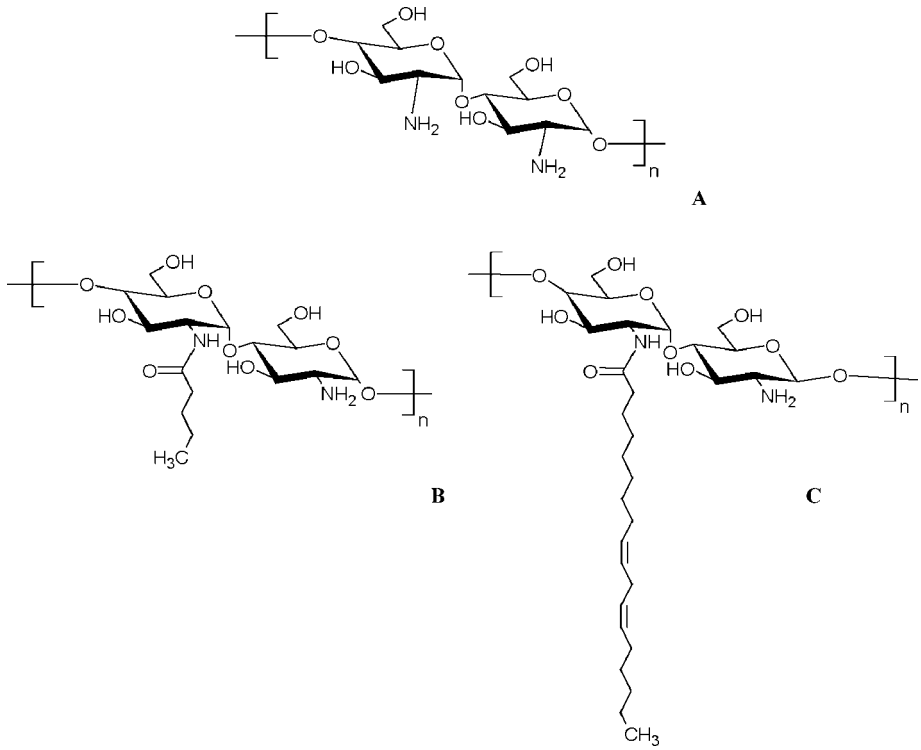

FIGURE 1. Structures of native and modified chitosan polymers: (A) native chitosan; (B) butyl-CHIT; (C) ALA-CHIT.

and hydrophobically modified chitosan polymers after they have been processed into 3D macroporous scaffolds. We also demonstrate the applicability of this technique to probe the chemical microenvironment surrounding the encapsulated enzyme after the polymer has been molded into 3D scaffolds. Specifically, MDH was labeled with the fluorophore AlexaFluor 546. Fluorescent dyes and/or the tagged enzymes were then added to separate solutions of chitosan polymer, two of which were hydrophobically modified with butyl alkyl chains and α-linoleic acid to possess amphiphilic micelles that could presumably encapsulate and retain the enzyme within unique chemical microenvironments (6). These solutions were then processed into 3D chitosan scaffolds using the thermally induced phase separation (TIPS) procedure (8, 11). The resulting degree of amphiphilicity and distribution of tagged enzymes throughout the polymer scaffold was then imaged using fluorescent confocal laser scanning microscopy.

MATERIALS AND METHODS

Medium molecular weight (MMW) chitosan was purchased from Sigma-Aldrich (Sigma-Aldrich, St. Louis, MO). Malate dehydrogenase (MDH) from porcine heart was obtained from Sigma-Aldrich (catalog no.18670, lot no. 62433). The enzyme was dialyzed against phosphate buffer (pH 7, 50 mM) to remove the magnesium salts used for stability in shipping. *N*-[3-(Dimethylamino)propyl]-*N*′-ethylcarbodiimide (EDC) and fluorescein sodium salt (95%) were purchased from Sigma-Aldrich and used without further modification. AlexaFluor 546 carboxylic acid succinimidyl ester was purchased from Molecular Probes (Invitrogen Corp., Carlsbad, CA).

Chitosan Pretreatment. To achieve a uniform degree of deacetylation (95%), MMW chitosan (CHIT; Figure 1A) was suspended in 45 wt % (11.25 M) NaOH and placed in an autoclave for 20 min at 121 °C (13). The resultant powder was then washed with 18 MΩ deionized water followed by phosphate buffer (pH 7, 0.1 M) before being dried in vacuo at 40 °C. The MMW chitosan was then purified of residual fluorescent contaminants by rinsing 1 g aliquots over vacuum filtration with 500 mL of 0.5 M NaOH followed by 500 mL of HPLC-grade methanol. The powder was then dried in vacuo (25 mbar) at 40 °C for 24 h.

Hydrophobic Modification. Butyl-modified chitosan (butyl-CHIT; Figure 1B) was prepared according to the method described by Klotzbach and co-workers (1). Specifically, 0.5 g of MMW chitosan was dissolved in 15 mL of a 1% acetic acid solution under rapid stirring until a viscous gel-like solution was achieved. A total of 15 mL of methanol was then added and the mixture allowed to stir for an additional 15 min, at which time 20 mL of butyraldehyde was added, followed immediately by the addition of 1.25 g of sodium cyanoborohydride. The gel-like solution was continuously stirred until the suspension cooled to room temperature. The resulting product was separated by vacuum filtration and washed with 150 mL increments of methanol. The hydrophobically modified chitosan was then dried in vacuo at 40 °C for 2 h, leaving a flaky white solid absent of any residual smell of aldehyde. A portion of this polymer was then suspended in 0.2 M acetic acid to create a 1 wt % solution and vortexed for 1 h in the presence of 2- and 5-mm-diameter yttria-stabilized zirconia oxide balls (Norstone, Wyncote, PA).

α-Linoleic acid modified chitosan (ALA-CHIT; Figure 1C) was prepared from a modified method of Liu and co-workers (14). Specifically, 1 g of MMW chitosan was dissolved in 100 mL of 0.2 M acetic acid and 85 mL of methanol under rapid stirring until a viscous solution was achieved. A total of 200 μL of α-linoleic acid was then added to the solution. A total of 10.5 mg of EDC (dissolved in 15 mL of methanol) was then added dropwise to the chitosan solution. The reaction was then covered and left to stir on a magnetic stirrer plate for 24 h. The resulting reaction mixture was then halted by pouring of the solution into 200 mL of a methanol/ammonia solution (7:3, v/v) under constant stirring. The precipitate was then rinsed with 1 L of distilled water followed by 500 mL of methanol and then 200 mL of ethanol over a vacuum filtration system. ALA-CHIT was then dried in vacuo at 40 °C for 1 week, yielding a flaky yellow solid.

Enzyme Labeling. To covalently bind the fluorophore to the enzyme, 280 μL of stock MDH (107 μM) and 30 μL of stock AlexaFluor 546 carboxylic acid succinimidyl ester (10 mM) were added to 690 μL of phosphate buffer (pH 8, 50 mM), yielding a final concentration of 30 μM MDH and 300 μM AlexaFluor 546, resulting in a 10:1 fluorophore-to-enzyme molar ratio. This solution was then incubated at 4 °C for 24 h with continuous stirring. To dilute away the unbound probe, the labeled enzyme was then purified by dialysis (MWCO 15000) against Tris buffer (50 mM, pH 7) for 24 h at 4 °C. The dialysis was repeated against fresh solutions of Tris buffer until no further change in the steady-state fluorescence polarization of the enzyme-containing fraction was measured. The polarization of AlexaFluor 546 in free solution was measured to be 0.04. When attached to a larger rotating body, MDH in this case, the polarization of the tagged enzyme solution eventually increased to and remained at 0.19, thereby confirming that the probe present in the fraction was covalently bound to the enzyme. The final fluorophore-to-enzyme molar ratio was measured to be 4:1 using Beers' law applied to spectrophotometric wavelength scans of the fluorophore-tagged enzyme solution.

Scaffold Preparation. Aqueous solutions of 1 wt % MMW chitosan were prepared by dissolving 1 g of the native or modified chitosan powder containing the immobilized enzyme in 100 mL of 0.2 M acetic acid, yielding a final polymer concentration of 40 μM at pH 2.5. In a previous study, we showed that the negatively charged fluorescein binds electrostatically to positively charged chitosan polymers (15). Consequently, 5 μL of 8 mM fluorescein (40 μM) was then added to each of the polymer solutions, resulting in a fluorescein-"stained" chitosan polymer. A total of 25 μL of the stock MDH/AlexaFluor 546 solution was then added to 225 μL of each of the stained chitosan and butyl- or ALA-modified chitosan solutions, respectively, yielding final concentrations of 10 μM AlexaFluor 546 and 3 μM MDH in a 36 μM solution of chitosan, butyl, or ALA-CHIT polymer. Polymer solutions stained with Nile Red were prepared as follows. Nile Red powder was dissolved in ethanol to a concentration of 438 μM. A total of 27.4 μL of this stock solution was then added to solutions of chitosan and butyl-modified chitosan, respectively, yielding final concentrations of 10 μM Nile Red in a 20 μM solution of chitosan or butyl-modified chitosan.

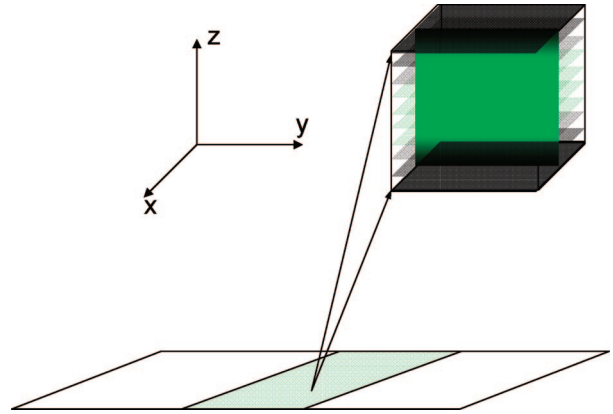

FIGURE 2. Geometrical representation of the slide and resultant images seen in Figures 4−6.

The scaffolds were prepared using a modified technique based on the procedure outlined by Yuan et al. (16, 17) and following discussions (P. Atanassov). A total of 50 μL of each solution described above was deposited using a micropipette onto a glass slide. To ensure that the surface of the glass slides were hydrophilic, they were cleaned and pretreated by submersion in a piranha solution (30% H_2O_2/96−98% H_2SO_4 mixed solution in a 1:3 ratio) followed by rinsing with deionized water and then air drying with filtered compressed air. The solution was then spread using an automated syringe pump (Cole-Parmer single-syringe infusion pump 74900) to drag a second glass slide over the meniscus at a rate of 1 μm/s for ∼30 min (16, 17). To prevent air drying during the coating, the entire process was conducted in a closed chamber kept at 20 °C and greater than 95% humidity. Once the coatings were set, the slides were then frozen at −20 °C for 1 h. Thereafter, the slides were vacuum-freeze-dried for 12 h.

Fluorescence Confocal Laser Scanning Microscopy. The resultant dried scaffolds were imaged using an Olympus Fluoview 1000 laser scanning confocal microscope. 3D images were reconstructed from individual layers in $x-y$ space (Figure 2). When the Nile Red stained scaffolds were examined, the fluorophores were excited at 515 nm. The resultant images were filtered using two band-pass filters of >650 and <620 nm, respectively. When the fluorescein-stained and enzyme-impregnated films were examined, the fluorophores were excited at 471 and 546 nm. The resultant images were filtered using two narrow-band-pass filters (490−520 and <620 nm) in order to determine the position of the chitosan polymer and MDH, respectively.

RESULTS AND DISCUSSION

Hydrophobic modification of the chitosan polymer is proposed to create amphiphillic micelles within the modified polymer (18, 19). Because the field of micellar enzymology has shown that amphiphilic micellar environments can cause superactivity, as well as thermal, pH, and solvent stability (20−22), Klotzbach and co-workers proposed that

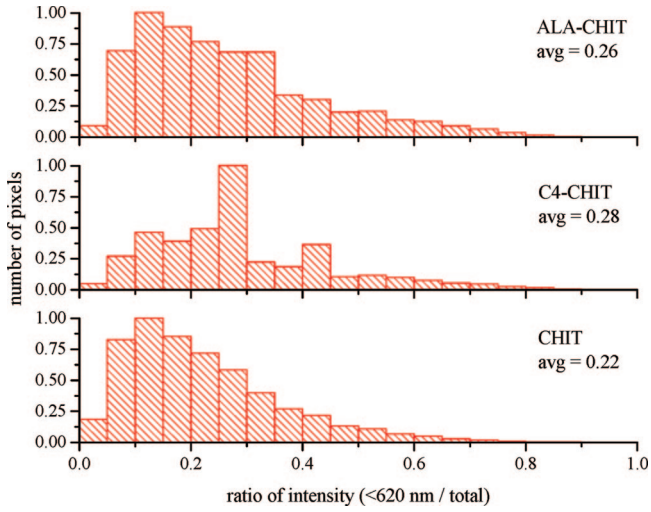

FIGURE 3. Distribution of the ratio of the emission intensity below 620 nm to the total emission intensity (each data point represents a single pixel in a 512 × 512 confocal image).

this micellar environment could be ideal for enzyme immobilization and stabilization (6). Cooney and co-workers further proposed that these modified polymers could be fabricated into 3D scaffolds in which the enzymes, encapsulated within the micelles, would line the surface of the scaffold macropores through which liquid-phase fuel could flow (8, 11). To test this theory, the distribution of these amphiphilic micelles can be confirmed using a polar probe, Nile Red, whose emission profiles vary depending upon the polarity of its immediate chemical microenvironment. In previous work, we used this approach to verify that the hydrophobic modification of chitosan does change the polymer's overall degree of amphiphilicity (15). In this presentation, we use this technique to more accurately assess the relative distribution of amphiphilic micelles within scaffolds fabricated from solutions of native as well as butyl or ALA chitosan. The results, plotted in Figure 3, are presented as the distribution of the ratio of the emission intensity below 620 nm to the total emission intensity. The emission intensity below 620 nm represents only that emission from Nile Red that results from its exposure to a more hydrophobic chemical microenvironment. The total emission represents the total sum of Nile Red's emission over all wavelengths, yielding contributions to Nile Red's emission from all chemical microenvironments (i.e., highly polar to highly nonpolar). Each data point represents a single pixel in a 512 × 512 confocal image. Consequently, the increase in the average of the total distribution from 0.22 to 0.26−0.28 for the modified chitosan polymers (relative to native chitosan) quantitatively suggests an increase in the hydrophobic nature of the chemical microenvironments provided by the amphiphilic micelles (i.e., by virtue of the fact that more pixels exhibited a larger intensity below 620 nm). The increase in the relative hydrophobic contribution to the amphiphilic nature of the micelles is likely the reason for the modified polymer's reported capacity for greater enzyme stabilization (3, 7).

It is assumed that an additional effect of the amphiphilic micelles is to immobilize the enzymes by encapsulation. If true, the enzymes should remain with the polymer during the TIPS process (i.e., freezing step). In other words, the amphiphilic micelles should encapsulate and retain the enzymes as they separate them, thereby "pulling" them along with the chitosan polymer as it separates from the water and eventually forming a precipitate (11). To test this theory, we mixed the AlexaFluor 546 labeled MDH in the various chitosan solutions and then formed chitosan scaf-

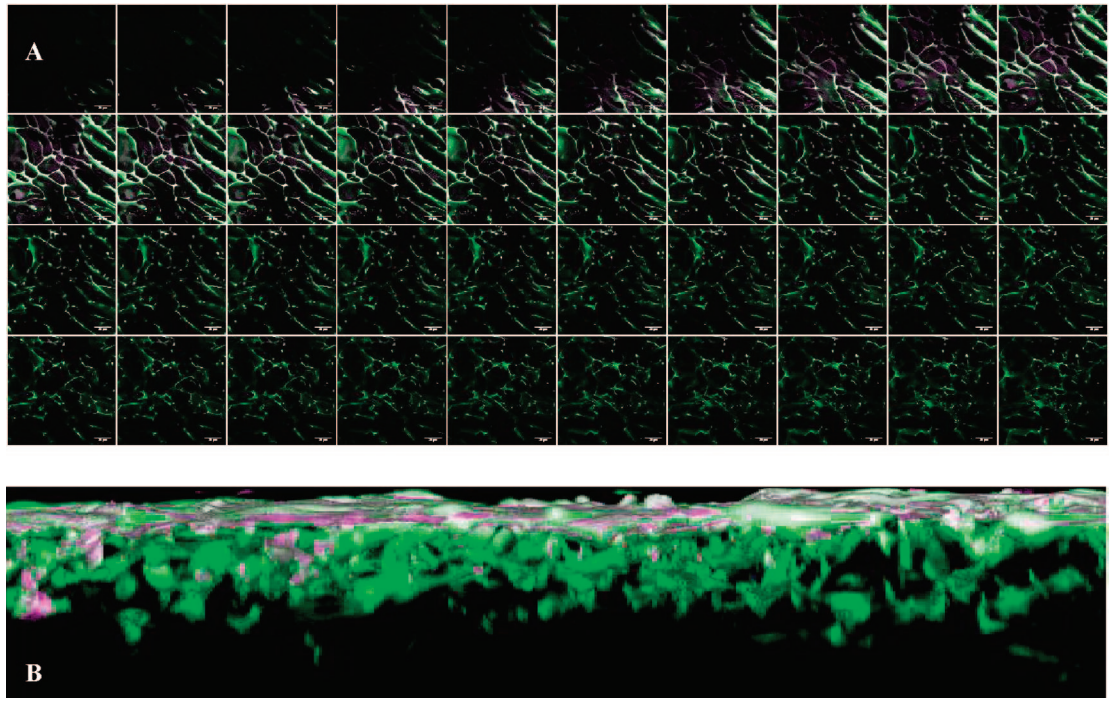

FIGURE 4. Enzyme distribution in native chitosan scaffolds stained with fluorescein (green) combined with AlexaFluor 546 stained MDH (purple): (A) *XY* cross sections of 0.82 μm between panels; (B) 3D projection of a ~80-μm-thick film, 0.414 μm between slices.

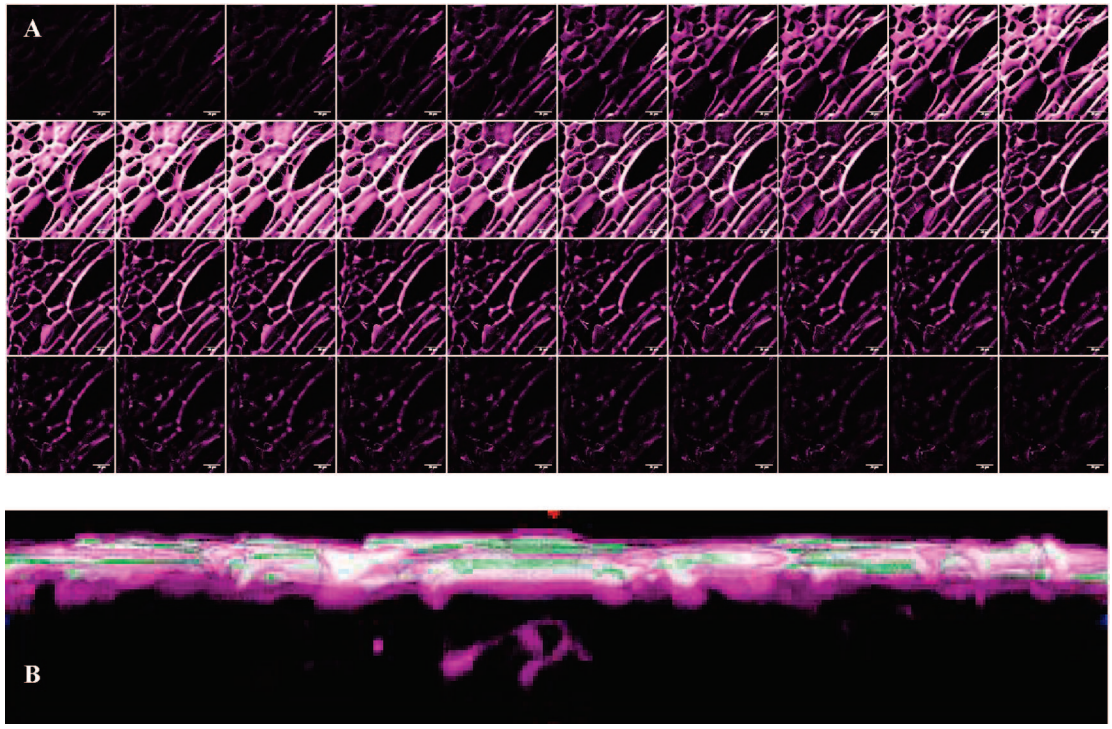

FIGURE 5. Enzyme distribution in butyl-modified chitosan scaffolds stained with fluorescein (green) combined with AlexaFluor 546 stained MDH (purple): (a) *XY* cross sections of 0.414 μm between panels; (b) 3D projection of a ~50-μm-thick film, 0.414 μm between slices.

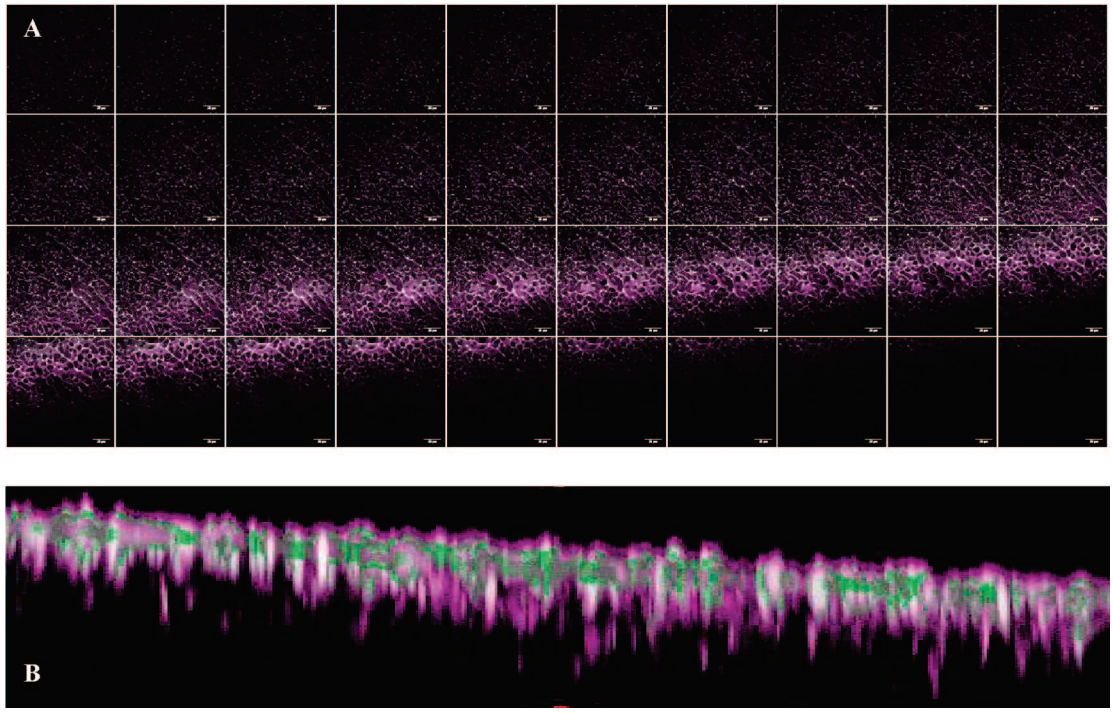

FIGURE 6. Enzyme distribution in α-linoleic acid modified chitosan scaffolds stained with fluorescein (green) combined with AlexaFluor 546 stained MDH (purple): (a) *XY* cross sections of 3.5 μm between panels; (b) 3D projection of a ~140-μm-thick film, 0.25 μm between slices.

folds using the previously described TIPS technique (8, 11) (Figure 4–6). Parts A and B of Figure 4 present the spatial distribution of enzyme immobilized within a scaffold fabricated from the native chitosan. The orientation of the individual confocal slices presented in Figure 4A is as presented in Figure 2. In part A, the distribution of chitosan precipitate (green) and tagged enzyme (purple) is presented in slices through the scaffold, starting from the top (upper left-hand side) and continuing down to the bottom (bottom right-hand side) in 0.414 μm increments. Clearly, the images suggest that more enzymes are located at the top of the scaffold than at the bottom and that no enzyme is located in the open pores. In part B, a 3D projection (i.e., reconstruction of the individual confocal slices) of a ~80-μm-thick scaffold is presented. Again, the localization of the enzyme to the surface of the chitosan scaffold is evident, suggesting

that the enzyme was not encapsulated by the polymer during the phase separation. The water remained during the phase-separation process, and the immobilization of enzyme occurs largely through the absorption of the enzyme to the surface of the precipitate.

By contrast, the distribution of MDH in the modified chitosan scaffolds, including both the butyl- and ALA-modified chitosan, shows a far more homogeneous distribution throughout the scaffold. For example, consider the butyl-CHIT scaffold presented in Figure 5. In part A, the distribution of enzyme throughout all slices (from top to bottom) is clearly evident. This feature is further illustrated in the profile presented in part B. The same spatial distribution of enzyme is evident in the ALA-CHIT scaffold, shown in Figure 6, although it appears to be more evenly distributed, a result that agrees with the hypothesis that amphiphilic micelles created by the fatty acid ALA side chains would be more likely to encapsulate and retain MDH because these fatty acids had been shown to provide MDH incorporation and stabilization in solution-based micelles (4). Combined, these observations support the hypothesis that the hydrophobic modification of the chitosan polymer does create amphiphilic micelles that can encapsulate the enzyme directly, thereby improving their retention and homogeneous distribution throughout the scaffold. We suspect that during the freezing process the encapsulated enzymes remain with the polymer as the water diffuses toward the growing ice crystals and the polymer phase dehydrates to a precipitate. Regardless of how accurate this initial assumption is, we have demonstrated that the described use of fluorescent microscopy permits an effective measurement of amphiphilicity of polymer micelles and the spatial distribution of enzymes encapsulated within them. This research tool permits a more accurate correlation of the effectiveness of the immobilization technique to measured the electrochemical performance of biocatalytic electrodes fabricated in either two or three dimensions. Although beyond the scope of this presentation, future collaborations with Atanassov and coworkers are planned to correlate the scaffold pore structure and enzyme distribution with the fabrication technique for thin films (16, 17).

Acknowledgment. Funding for this work was provided by the Office of Naval Research (Contract N0014-01-1-0928) through the Hawaii Environmental and Energy Technology (HEET) initiative (Richard Rocheleau, PI) and from the AFOSR Multidisciplinary University Research Initiative program (Award FA9550-06-1-0264) under the Fundamentals and Bioengineering of Enzymatic Fuel Cells award (P. Atanassov, PI). The authors also gratefully thank Rosalba Rincon and Plamen Atanassov for their time and discussions on transferring the polymer film coating methodology.

REFERENCES AND NOTES

(1) Klotzbach, T.; Watt, M.; Ansari, Y.; Minteer, S. D. *J. Membr. Sci.* **2006**, *282* (1−2), 276–283.
(2) Minoofar, P. N.; Dunn, B. S.; Zink, J. I. *J. Am. Chem. Soc.* **2005**, *127* (8), 2656–2665.
(3) Bru, R.; Sanchez-Ferrer, A.; Garcia-Carmona, F. *Biochem. J.* **1995**, *310*, 721–739.
(4) Callahan, J. W.; Kosicki, G. W. *Can. J. Biochem.* **1967**, *45*, 839–851.
(5) Moore, C. M.; Akers, N. L. *Biomacromolecules* **2005**, *5*, 1241–1247.
(6) Klotzbach, T. L.; Watt, M.; Ansari, Y.; Minteer, S. D. *J. Membr. Sci.* **2008**, *311* (1−2), 81–88.
(7) Cooney, M. J.; Svoboda, V.; Lau, C.; Martin, G. L.; Minteer, S. D. *Energy Environ. Sci.* **2008**, *1* (3), 320–337.
(8) Cooney, M. J.; Lau, C.; Windmeisser, M.; Liaw, B. Y.; Klotzbachb, T.; Minteer, S. D. *J. Mater. Chem.* **2008**, *18*, 667–674.
(9) Schuhmann, W. *Biosens. Bioelectron.* **1995**, *10* (1−2), 181–193.
(10) Lau, C.; Cooney, M. J.; Atanassov, P. *Langmuir* **2008**, *24* (13), 7004–7010.
(11) Cooney, M. J.; Petermann, J.; Lau, C.; Minteer, S. D. *Carbohydr. Polym.* **2008**, in press.
(12) Konash, A.; Cooney, M. J.; Liaw, B. Y.; Jameson, D. M. *J. Mater. Chem.* **2006**, *16*, 4107–4109.
(13) Sjoholm, K. H.; Cooney, M. J.; Minteer, S. D. *Carbohydr. Polym.* **2008**.
(14) Liu, C. G.; Desai, K. G. H.; Chen, X. G.; Park, H. J. *J. Agric. Food Chem.* **2005**, *53* (2), 437–441.
(15) Martin, G. L.; Ross, J. A.; Minteer, S.; Cooney, M. J. *Carbohydr. Polym.* **2008**.
(16) Yuan, Z.; Burckel, D. B.; Atanassov, P.; Fan, H. *J. Mater. Chem.* **2006**, *16*, 4637–4641.
(17) Yuan, Z.; Petsev, D. N.; Prevo, B. G.; Velev, O. D.; Atanassov, P. *Langmuir* **2007**, *23* (10), 5498–5504.
(18) Jiang, G.-B.; Quan, D.; Liao, K.; Wang, H. *Carbohydr. Polym.* **2006**, *66* (4), 514–520.
(19) Esquenet, C.; Terech, P.; Boue, F.; Buhler, E. *Langmuir* **2004**, *20* (9), 3583–3592.
(20) Martinek, K.; Klyachko, N. L.; Kabanov, A. V.; Khmelnitsky, Y. L.; Levashov, A. V. *Biochim. Biophys. Acta* **1989**, *981* (2), 161–172.
(21) Martinek, K.; Klyachko, N. L.; Levashov, A. V.; Berezin, I. V. *Dokl. Akad. Nauk SSSR* **1983**, *269* (2), 491–493.
(22) Martinek, K.; Pshezhetskii, A. V.; Merker, S.; Pepanyan, G. S.; Klyachko, N. L.; Levashov, A. V. *Biokhimiya* **1988**, 53.

AM800077T